Changes in the deep ocean conveyor and eolian sediment transport caused by meltwater events in high latitudes

Bernd J. Haupt[1] and Dan Seidov[2]

Earth & Mineral Science Environment Institute, Pennsylvania State University
2217 Earth–Engineering Science Bldg., University Park, PA 16802–6813, USA

[1]e–mail: bjhaupt@essc.psu.edu; URL: http://www.essc.psu.edu/~bjhaupt
[2]e–mail: dseidov@essc.psu.edu; URL: http://www.essc.psu.edu/~dseidov

Abstract

The major unknown in paleoceanographic modeling is whether changes of sedimentation patterns can be linked to long–term variability of the global ocean water mass motion in numerical experiments. On a millennium time scale, the most dramatic changes of the ocean circulation are caused by meltwater events in the high latitudes. It is thought that some of these events were strong enough to halt or even reverse the thermohaline conveyor in the Atlantic Ocean. Eolian sediment can be treated as a tracer of the ocean currents, similarly to other passive tracers. The advantage of using inorganic sediment as an ocean tracer is that its distribution can be read in geologic record. A combination of an ocean global circulation model (OGCM) and a large–scale 3–D sediment transport model is employed in this study in order to simulate the global ocean thermohaline conveyor and distribution of the global eolian sediment accumulation patterns. Experiments with a realistic present–day eolian dust source at the sea surface have been carried out. First results are encouraging and indicate that this approach can substantially increase our confidence in paleoceanographic simulations.

Introduction

Over the past several decades, modeling glacial–to–interglacial changes of the global ocean thermohaline conveyor and its global impact of on the oceanic sedimentary system provides, together with the oceanic sediment collection, a growing opportunity to address quantitatively a number of fascinating paleoceanographic problems. However, most of the existing sedimentation models are two–dimensional and are designed for small basins, targeting specific features such as alluvial or deltaic basin fill (cf. *Ericksen et al.* [1989]; *Tetzlaff and Harbaugh* [1989]; *Bitzer and Pflug* [1990]; *Paola et al.* [1992]; *Syvitski and Daughney* [1992]; *Cao and Lerche* [1994]; *Slingerland et al.* [1994]). Usually, such models are not suitable for assessing the impact of global climate change on the ocean sediment drifts on millennial and longer time scales. As a rule, their sediment transport is gravity–driven, with the sediment load proportional to the basin slope, water discharge, and diffusion coefficient (e.g., *Granjeon and Joseph* [1999]). To address the

linkages between sedimentation and deep–ocean circulation we use a three–dimensional coupled ocean circulation–ocean sedimentation model, with the only 3–D global ocean sedimentation model available to date [*Haupt et al.*, 1994]. Our objective is to assess whether it is possible to trace the changes in the total terrigenous sedimentation rates induced by millennium–scale changes of the ocean currents. As an example, we model the global ocean thermohaline conveyor at present–day (MOD), at the last glacial maximum (LGM) (22–18 ka BP), and at a subsequent Heinrich–type meltwater event (MWE) near 13.5 ka BP. The global oceanic thermohaline circulation, (e.g., *Stommel* [1958]; *Gordon* [1986]; *Broecker and Denton* [1989]; *Broecker* [1991]), which is driven by deepwater production in the high–latitudes, is very sensitive to the changes in freshwater fluxes in the high–latitudinal North Atlantic. If these freshwater–induced changes in deep–sea currents led to noticeable changes in sedimentation patterns, they can probably be traced in experiments with the coupled circulation–sedimentation model. The geologic record indicates that at least in some regions the sediment patterns are indicative of climate change and perhaps can be used for achieving our goals.

This study expands on previous works by *Seidov and Haupt* [1997] and *Seidov and Haupt* [1999] by using realistic present–day eolian dust patterns [*Rea*, 1994] at the sea surface with the objective of predicting more realistic sedimentation pattern.

Numerical Setup of Experiments and Data

In order to compare glacial–to–interglacial changes in oceanic sediment transport, we use a combination of an OGCM and an off–line coupled three–dimensional large–scale sediment transport model. To test the effect of glacial–to–interglacial global thermohaline circulation (THC) changes on the deep–sea sedimentation three numerical experiments were carried out They were completed using GFDL MOM version 2.2, a well documented and extensively utilized ocean circulation model [*Bryan*, 1969; *Cox*, 1984; *Pacanowski et al.*, 1993; *MOM-2*, 1996]. In our control experiment (MOD), the upper layer of the ocean temperature and salinity are restored to the present–day sea surface climatology that is to sea surface temperature (SST) and sea surface salinity (SSS). As wind stress field the Hellerman–Rosenstein [*Hellerman and Rosenstein*, 1983] annual mean wind stress was used. To address circulation changes during the glacial–to–interglacial transition we have chosen two experiments from the late Quaternary as examples: (1) a scenario for the LGM and (2) a Heinrich–type meltwater event (MWE), when the first strong deglaciation of the Barents shelf occurred. Table 1 gives a detailed outline of the used sea surface boundary conditions (SST and SSS). The wind stress field was taken from the Hamburg atmospheric circulation model, which was forced with glacial sea surface climatology [*Lorenz et al.*, 1996]. We use the same wind stress for both time slices, LGM and MWE, although it has been shown that the alteration of wind stress in the Southern Ocean can by itself cause changes in the Atlantic deep–water circulation

(e.g., *Toggweiler and Samuels* [1995]; *Rahmstorf and England* [1997]). However, we focus on the meltwater control, which provides a distinctive signature of glacial–to interglacial changes. Our meltwater event scenarios are designed to mimic real meltwater events caused by iceberg flotillas from either the Laurentide Ice Sheet (e.g., *Ruddiman and McIntyre* [1981]) or the Barents Ice Shelf (e.g., *Sarnthein et al.* [1994]). As these events substantially altered the THC/deep–ocean circulation, we anticipate that they led to abrupt and noticeable changes in sedimentation patterns.

Table 1. Sea surface temperature and salinity in numerical experiments

Exp.	SST	SSS
MOD	SST from present-day sea surface climatology [*Levitus and Boyer*, 1994].	SST from present-day sea surface climatology [*Levitus et al.*, 1994].
LGM	*CLIMAP* [1981] SST is used everywhere except for the NA to the north of 50°N and east of 40°W, where the data from *Schulz* [1994], summarized in *Sarnthein et al.* [1995] and processed in *Seidov et al.* [1996] replace the CLIMAP data.	The present day SSS was increased by 1 psu according to *Duplessy et al.* [1991]; in the NA, to the north of 10°N, the data set from *Duplessy et al.* [1991] and *Weinelt* [1993], summarized in *Sarnthein et al.* [1995] and processed in *Seidov et al.* [1996].
MWE	As for the LGM except for the NA to the north of 50°N and east of 40°W, where SST from *Weinelt* [1993], summarized in *Sarnthein et al.* [1995] and processed in *Seidov et al.* [1996] replace the LGM SST.	As in LGM, except for the NA north of 50°N and east of 40°W where SSS from *Weinelt* [1993], summarized in *Sarnthein et al.* [1995] and processed in *Seidov et al.* [1996] replace the LGM surface salinity.

Here: MOD is for present–day scenario (modern); LGM = last glacial maximum; MWE = meltwater event (see text); SST = sea surface temperature; SSS = sea surface salinity; CLIMAP = Climate Long-Range Investigation Mapping and Prediction; NA = North Atlantic.

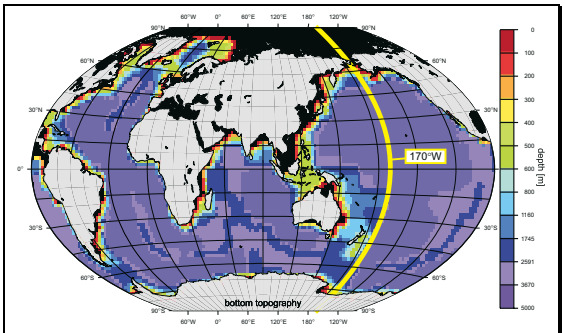

Figure 1. Model bathymetry with a horizontal grid spacing of 6°x4° and 12 unequally spaced vertical layers. The bathymetry is derived from the [*ETOPO5*, 1986] data set and represents a smoothed version of the real World Ocean bottom topography.

[1986] data set representing a smoothed version of the real World Ocean bottom topography (Figure 2). *Cox* [1989] and *Toggweiler et al.* [1989] have shown that

In order to facilitate multiple millennium–scale runs, we use a relatively coarse global model domain with a horizontal grid spacing of 6°x4° and 12 unequally spaced vertical layers as shown in Figure 1. The bathymetry is derived from the *ETOPO5*

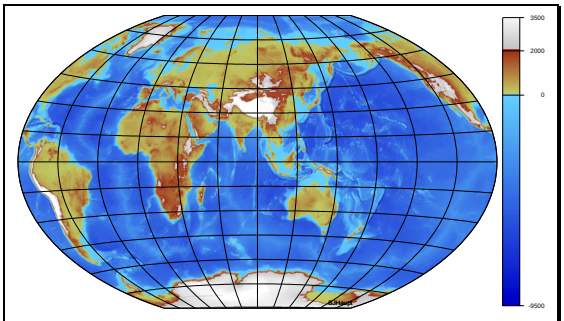

Figure 2. Real World Ocean bathymetry [*ETOPO5*, 1986].

MOM is capable of reproducing the rates of deep–water production and thermohaline overturning fairly well in the framework of a rather coarse horizontal resolution, a result that has been confirmed by many other recent modeling efforts that target long–term climate change (e.g., *Toggweiler et al.* [1989]; *Manabe and Stouffer* [1995]; *Rahmstorf* [1995]; *Seidov and Haupt* [1999]).

However, the use of a coarse resolution, although well suited for a scenario–type study as reported here, has its shortcomings, especially in resolving coastal geometry. For example, Iceland is represented by a seamount in the model bottom topography. Therefore, velocity vectors, water mass transports, and non–zero sedimentation rates are artifacts at the exact position of this island. There are some other locations where coarse resolution leads to distorted land–sea distributions on a scale smaller than the grid step. However, major features of large–scale thermohaline circulation are resolved.

A key question is whether a coarse resolution model is capable to distinguish between 'sediment drifts', or if the results of the sedimentation models only indicate regions where they might occur. It is unquestionable that such a coarse resolution does not allow the identification of single known sediment drifts and waves, respectively, especially when they are in close vicinity. In spite of this *Haupt et al.* [1994], *Haupt* [1995], *Haupt et al.* [1995], *Stattegger et al.* [1997], *Haupt and Stattegger* [1999], *Haupt et al.* [1999], and *Seidov and Haupt* [1997] showed in previous studies with earlier versions of both OGCM and sediment transport model at much higher horizontal resolutions, 0.5°x0.5° and 2°x2° respectively, that the sediment transport model is capable of reproducing and distinguishing between 'small' drifts in the North Atlantic and around Iceland. Therefore, we mainly focus on the impact of glacial–to–interglacial changes in deep–ocean currents on the large–scale sedimentation patterns, especially in the areas of higher sediment accumulation, rather than on identification of single sediment drift bodies.

All OGCM runs are 2000 model years long, with a 5–fold acceleration in the deep layers (which means that the deep ocean is effectively run for 10,000 years). All runs reached a complete steady state. For example, the global temperature and salinity changes for the last 100 model years are less than 10^{-4} °C and 10^{-5} psu, respectively. The tracer time step length is 86400 s (1 day) and the time step length for velocity is 250 s. A more detailed view of the OGCM results can be found in *Seidov et al.* [2001] and *Haupt et al.* [2001].

We assume that after a spin–up from one steady state to another (for example, a glacial or a meltwater state) the deep–ocean circulation is unchanged on those timescales and one can use the steady state velocity and thermohaline fields to calculate sediment distribution employing the off–line coupled large–scale dynamic sediment transport model SEDLOB (SEDiment transport in Large Ocean Basins). Major features

of SEDLOB are given by *Haupt et al.* [1994]; the most recent and detailed descriptions of this model are given by *Haupt et al.* [1999] and *Haupt et al.* [2001].

Thus, the OGCM provides velocity, temperature, salinity, and convection depths (in the locations where convection occurs due to hydrostatic instability) at steady state, which enter SEDLOB as external parameters. Internal variable parameters that are specified in SEDLOB are the sediment properties, including the sediment sources, the sinking velocity (0.05 cm s^{-1} = 43.2 m d^{-1} after *Shanks and Trent* [1980]), the density (ρ_s = 2.6 g cm^{-3}) and porosity (γ = 0.75) of sediment, grain size and sedimentological grain diameter, and form factor of sediment particles (FF = 0.7) [*Zanke*, 1982]. The sediment source properties as well as the sediment material entry are identical for all experiments. Although the prescribed sediment source can include any kind of inorganic sediment including eolian dust, ice–rafted debris and riverine sediment input, we prescribe at this stage of research for simplification only inorganic eolian dust particles at the sea surface. Neglecting the influence of biochemical processes allows us to focus on non–biogenic and non–dissolvable sediment because it behaves as a passive tracer. Thus, the mass of sediment covering the seafloor depends only on the balance of sources and sinks, whereas the spatial variation of the sedimentation rate depends on the circulation pattern and particle grain size. In the absence of the ocean currents (i.e., when sediment particles only settle downward and are not transported by the ocean flow; there was a test run with all velocities set to zero in SEDLOB), the pattern of sediment deposition rates repeats the pattern of the prescribed dust input at the surface. With currents switched on, the spatial structure of deposition is entirely determined by the transport, erosion, and re–deposition of sediment by the three–dimensional ocean currents.

Further simplifications that are described in more detail by *Haupt et al.* [2001] are:

1. The disregard of biologically mediated aggregations of upper–ocean–generated particles that settle with bulk speeds up to 200 m d^{-1} much faster than individual fine particles [*Honjo*, 1996];
2. The disregard of plate tectonic processes such as continental displacement, subsidence, subduction, and sea–floor spreading, as well as sediment compaction because they occur on much longer time scales than millennial–scale glacial cycles that we can simulate with reasonable computer resources;
3. The disregard of glacial sea level lowering of approximately 100 m during the LGM [*Fairbanks*, 1989] including glaciation of shelf areas down to 200 m [*CLIMAP*, 1981; *Lehman*, 1991; *Mienert et al.*, 1992] because its effect on the global thermohaline circulation is minor.
4. The use of only the present–day eolian dust source (after *Rea* [1994], Figure 3) at the sea surface for all experiments.

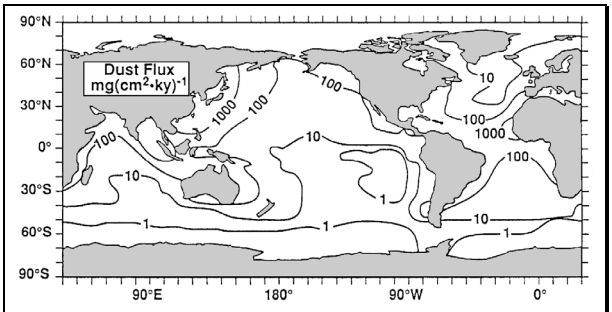

Figure 3. Estimate of the rate of deposition of mineral dust based on consideration of atmospheric transport (reproduced from [*Rea*, 1994], after [*Duce et al.*, 1991]).

Regarding the use of present–day source for all three time slices at this stage of research is justified by the following. Although there is some basic knowledge about some of the features of the aridity, wind speed and direction, and eolian sediment availability in many locations for the LGM (with much less knowledge existing for the MWE), there still is a great deal of uncertainty in mapping the spatial distribution of eolian dust. Given this uncertainty, the use of the same realistic present–day eolian dust patterns (after *Rea* [1994]) for all three time slices has been thus considered, in this preliminary study, a better alternative to introducing more uncertainty in the source of sediment. Having the same surface sediment source, the modeled sedimentation rates illustrate exclusively differences between the near–bottom currents during the three glacial–to–interglacial modes.

All experiments with SEDLOB, one for each climate state, were run for 1000 years without deep–ocean acceleration. An important fact is that it is not possible to run SEDLOB to a steady state because the forward time integration leads in every time step to continuous changes in bottom slope. As a result the critical velocities for initiating bed and suspension loads change as well, altering both bed and suspension load transports. These changes influence the maximum possible sediment concentrations and transport in the fluid because they are dependent. This may be viewed as the equivalent of changing sediment availability in every time step.

Results and Discussion

The effect of climate variability via the global thermohaline circulation is directly linked to deep–sea sedimentation processes, which means that each climatic phase throughout earth's history leaves its characteristic imprint at the sea floor. The comparison of modeled sediment deposition rate changes will provide a better understanding of the glacial–to–interglacial variability of thermohaline currents, and help to identify the regions of the world ocean that are most sensitive to glacial and meltwater impacts.

In the first part of this section, three different climates, i.e., MOD, LGM, and MWE, are compared by comparing the THC parameters, such as intensity of meridional circulation, oceanic meridional heat transport, thermohaline structure of the ocean, deep–water production rates, and calculated water transport through vertical sections in certain areas in the global ocean. In the second part of the section, simulated sediment accumulation rates are compared with the available geologic record. In the following section, we try to link the glacial–to–interglacial variability of the deep ocean circulation to the changes in sediment deposition and to show that sediment transport modeling can be used as an instrument for validating the ocean paleocirculation modeling.

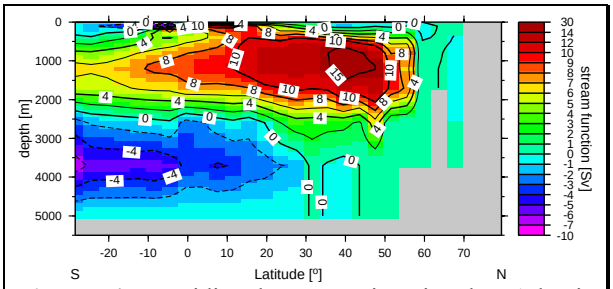

Figure 4. Meridional overturning in the Atlantic Ocean for the present–day experiment (MOD) (in Sv; 1 Sv = 10^6 $m^3 s^{-1}$) The positive values depict clockwise motion while negative values depict counterclockwise motion. The Atlantic overturning is valid only within this ocean's geographical boundary (with meridional walls at both sides; therefore the area south of 30ºS is not shown).

One of the key elements of the present–day meridional ocean circulation is the southward North Atlantic Deepwater (NADW) outflow from the convection sites in the Norwegian–Greenland Seas and northern North Atlantic (NNA). Figure 4 shows the meridional overturning (in Sverdrups (Sv); 1 Sv=10^6 m^3 s^{-1}) in the Atlantic Ocean in a vertical plane. The stream function is positive if the water motion is clockwise while negative values show counter clockwise water transport. The Atlantic overturning is shown only north of 30ºS because the meridional overturning can only be determined either for global flow with cyclic conditions or with meridional boundaries. In our present–day (MOD) control run the NADW, which has a production rate of approximately 15 Sv (compare also Figure 5), penetrates deep enough to set forth the deep–ocean conveyor. This result agrees well with water transport estimations of *Schmitz* [1995]. The Antarctic Bottom Water inflow into the Atlantic Ocean is about 8 Sv, the NADW outflow across 30ºS is more than 10 Sv (see Table 2). This fits the range given by different models, which are known to be sensitive to even small changes in bottom topography, especially in the Drake Passage area (see discussion by *Toggweiler and Samuels* [1995] and by *Rahmstorf and England* [1997]), and vertical diffusivity [*Bryan*, 1987; *Cummins et al.*, 1990].

Table 2. Meridional overturning in the Atlantic Ocean (north of 30ºS) in Sv (1 Sv = 10^6 m^3 s^{-1})

Exp.	NADW production	NADW outflow at 30ºS	AABW inflow at 30ºS
MOD	15	10	6–8
LGM	8	6	4
MWE	–	-2	3–4

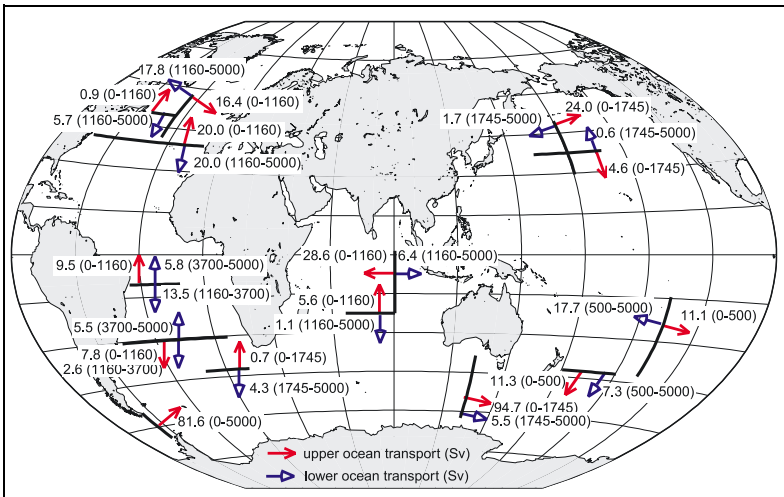

Figure 5. Present–day (MOD) water mass transport in Sv (1 Sverdrup (Sv) = 10^6 $m^3 s^{-1}$) across chosen meridional and zonal vertical sections for different depths in different oceans. Primarily, the transports in the upper and deep ocean are shown; in cases when upper and intermediate water movement essentially differs, the transports in three layers are shown to differentiate between the upper, intermediate–to–deep, and deep–to–abyssal flows.

Figure 6 presents the northward heat flux in the Atlantic Ocean and for the global ocean, respectively. The cross–equatorial northward heat flux shows how strongly do ocean currents warm the Northern Hemisphere.

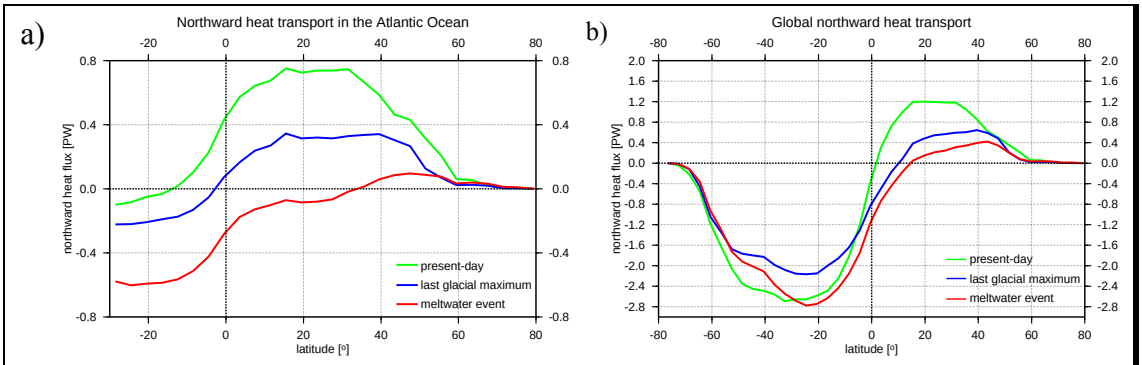

Figure 6. Northward oceanic heat transport (in PW; 1 PW = 10^{15} W) in the (a) Atlantic Ocean and (b) global ocean, respectively.

Meltwater impacts in the Northern Hemisphere caused largely by sea ice melting lead to a weakening of the THC as soon as a sufficient number of icebergs travel to the main convection sites in the North Atlantic reducing or even stopping the NADW production (Table 2) within a matter of years. However, it may take hundreds of years to transport the signal of a reduced density of the NNA's sea surface waters into the deep ocean [*Broecker*, 2000]. The weakening (LGM) and collapse (MWE) of the THC is shown in Figure 7. The depth and intensity of the NADW outflow and overall circulation configurations in the present–day and LGM runs, especially in the Southern Ocean, match those by *Winguth et al.* [1999] (who provide a comparison of modeled circulation with reconstructed biogeochemical tracers). The weakening of THC leads in the Atlantic Ocean to a reduced cross–equatorial northward oceanic heat flux (Figure 6a), which even reverse its sign in the MWE case leading to a southern versus northern (normal) 'heat piracy' [*Seidov and Maslin*, 2001]. Although it could be thought that the impact of these changes of the meridional overturning regime is constrained to the Atlantic branch of the THC, our model confirmed the concept of global impact of these changes. The THC, also known as a 'salinity conveyor belt' [*Stommel*, 1958; *Broecker and Denton*, 1989;

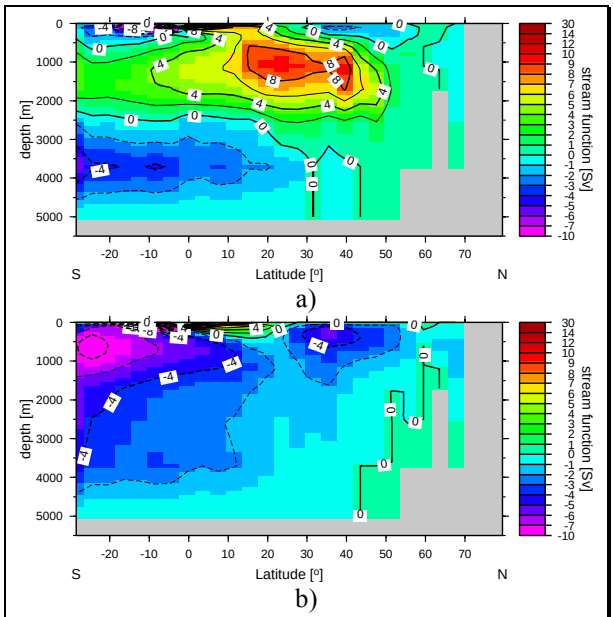

Figure 7. As in Figure 4 for (a) LGM and (b) MWE.

Broecker, 1991], is driven by deepwater production in the high–latitudes, especially by the production of NADW, a problem that has been addressed in several studies (e.g., *Manabe and Stouffer* [1988, 1995, 1997], *Maier-Reimer et al.* [1991], *Seidov and Haupt* [1999]; *Seidov and Maslin* [1999]). The impact of the weakened THC during the glacial/interglacial periods (Figure 7) can be clearly traced to the Indian and Pacific Oceans (compare Figure 5 with Figure 8). The model confirms that cooling of the Pacific Ocean's intermediate and deep water is caused by weakening of the THC during both LGM and MWE (Figure 9).

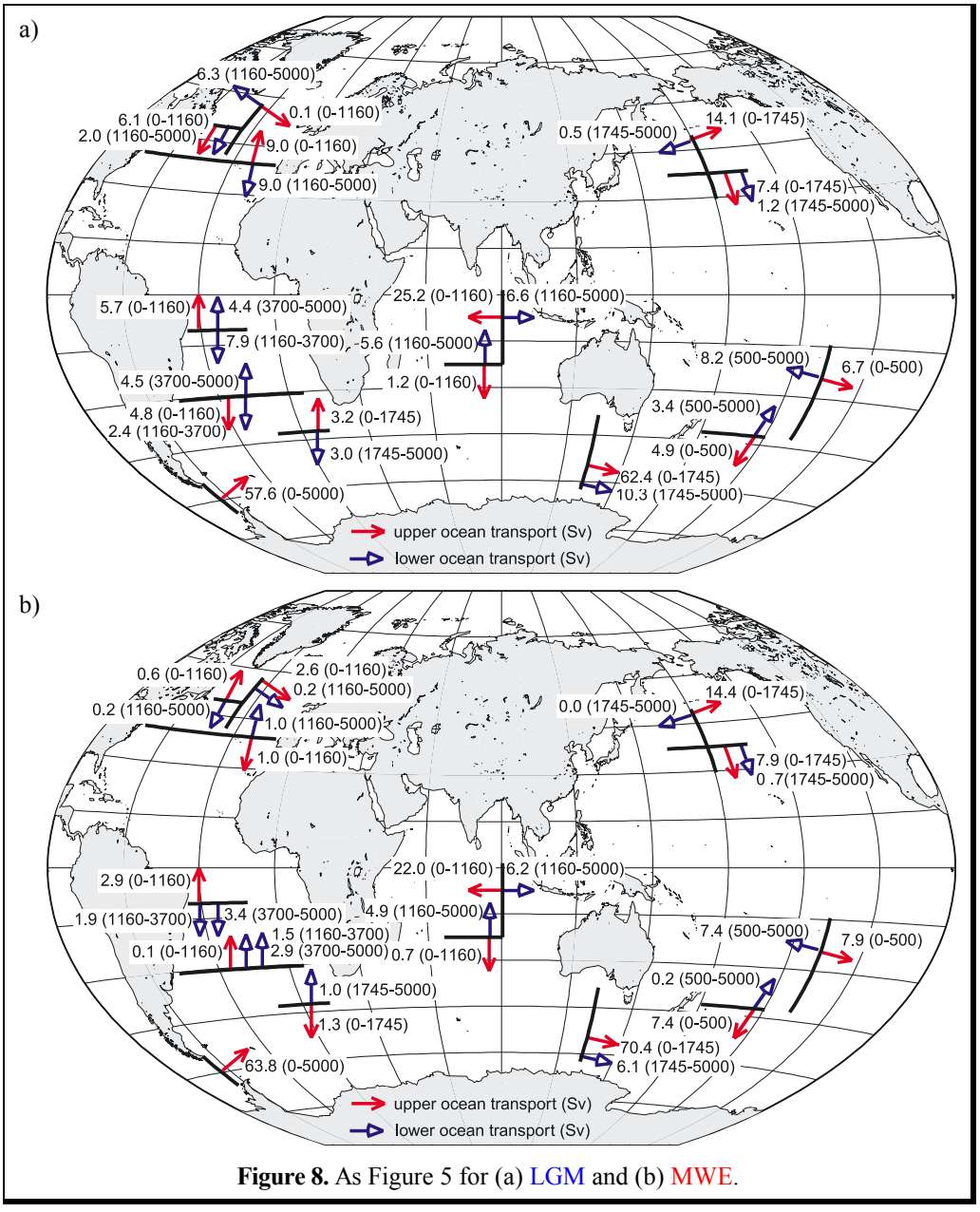

Figure 8. As Figure 5 for (a) LGM and (b) MWE.

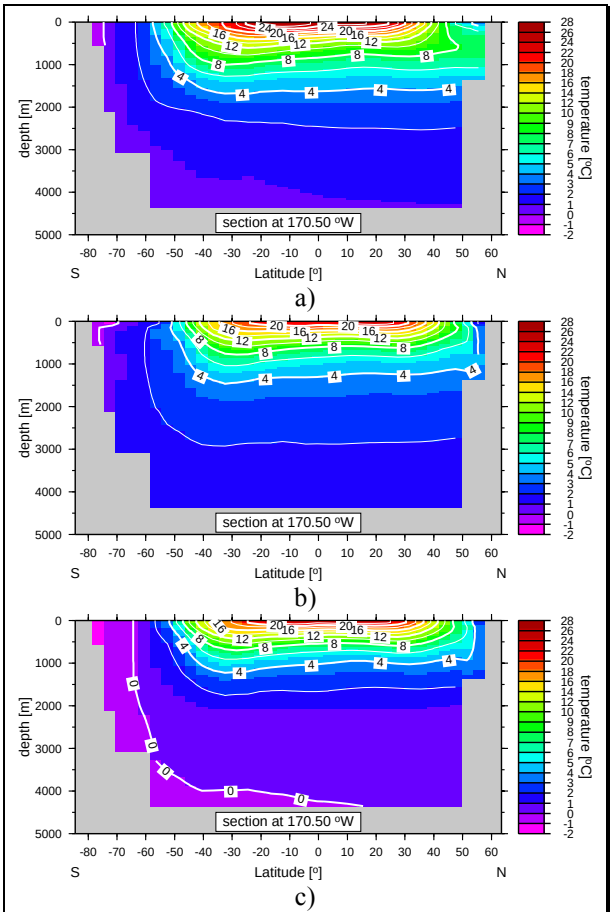

Figure 9. Temperature sections in the Pacific Ocean at 170°W (see arc in Figure 1): (a) MOD, (b) LGM, and (c) MWE

The dynamics of sediment transport correlates well with the major THC changes. Figure 10 depicts the modeled changes of sediment deposition rates for the three time slices MOD, LGM, and MWE. It must be emphasized that the model still does not represent the details of a real world sedimentation pattern. Consequently, the modeled sediment rates do not look like any real map of sediment accumulation rates despite the use of realistic present–day eolian dust load [*Rea*, 1994] at the sea surface. Very important riverine source of inorganic sediment can dramatically change local sedimentation rates. This sediment supply has not yet been included in the model. However, the areas of strong impact of the circulation on the sediment transport can be easily identified in Figure 10.

As the absolute rates of sedimentation are biased due to absence of the riverine discharge, they cannot be used in a direct model–observation comparison. Yet the analysis of areas with higher sedimentation rates helps to verify changes in deep–ocean water transports reflected in sediment drifts and sediment waves [*Flood and Shor*, 1988]. The presence of known sediment drifts (Figure 11), revealed by fine–grained sediment, has often been used as an indicator of steady, sediment–laden flows. This correlation is useful for understanding the role of deep–ocean currents in creating and maintaining large–scale sediment drifts.

McCave and Tucholke [1986] link high sedimentation rates to areas of maximum kinetic energy in the western boundary currents. Our present–day simulation also shows increased sedimentation in the western North Atlantic, within the southward–flowing deep western–boundary current. Moreover, our model predicts sediment drifts south of Iceland, in the Caribbean Sea, and in most other key regions, including the southern part of the Argentine Basin, the Cape and Agulhas Basin, and areas east of Australia and New Zealand, which are under the control of the East Australian Current. According to *Carter et al.* [1996] the oceanic sedimentary system on eastern New Zealand margin was continuously supplied with sediment for at least 10 My (see also sedimentation pattern in this

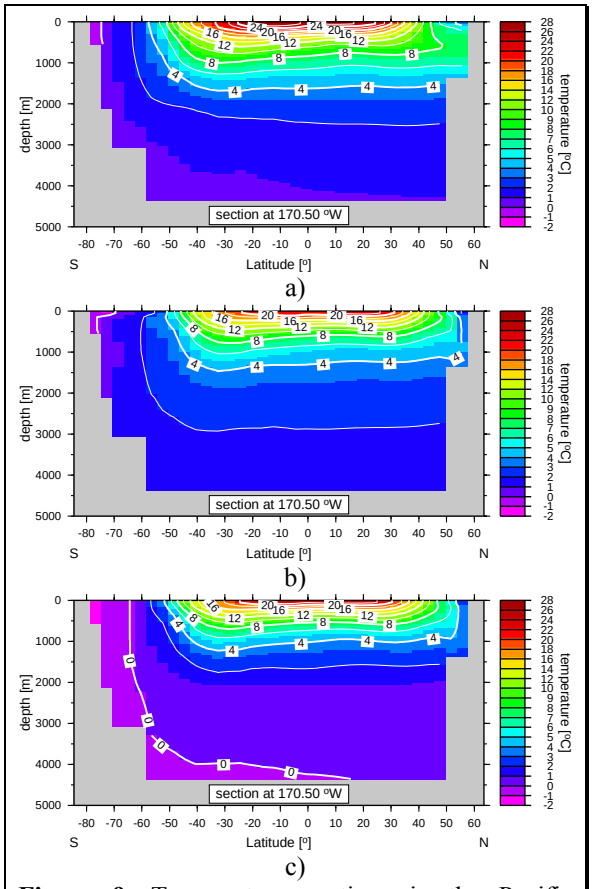

Figure 9. Temperature sections in the Pacific Ocean at 170°W (see arc in Figure 1): (a) MOD, (b) LGM, and (c) MWE.

region for LGM (Figure 10b) and MWE (Figure 10c)). Locations of high sediment deposition rates of modeled sedimentation patterns are generally in a good agreement with the current knowledge of the dynamics of inorganic sediment in these areas [*McCave and Tucholke*, 1986; *Bohrmann et al.*, 1990]. Other areas with increased sedimentation rates that emerged in our experiments are observed in the southern part of the Argentine Basin in the area of the Falkland Escarpment (~50ºS, ~55–40°W). *Flood and Shor* [1988] link these drifts, in particular the Zapiola Drift, to the Falkland current.

In the Indian Ocean SEDLOB gives high accumulation rates in the Cape and Agulhas Basins, which is in agreement with observations (e.g., *Hollister and McCave* [1984]; *Faugeres et al.* [1993]). The map of suspended material load by *Hollister and McCave* [1984] corresponds to the high kinetic energy of surface currents and the spread of deep–ocean cold water. However, predicted sedimentation rates for the Arabian

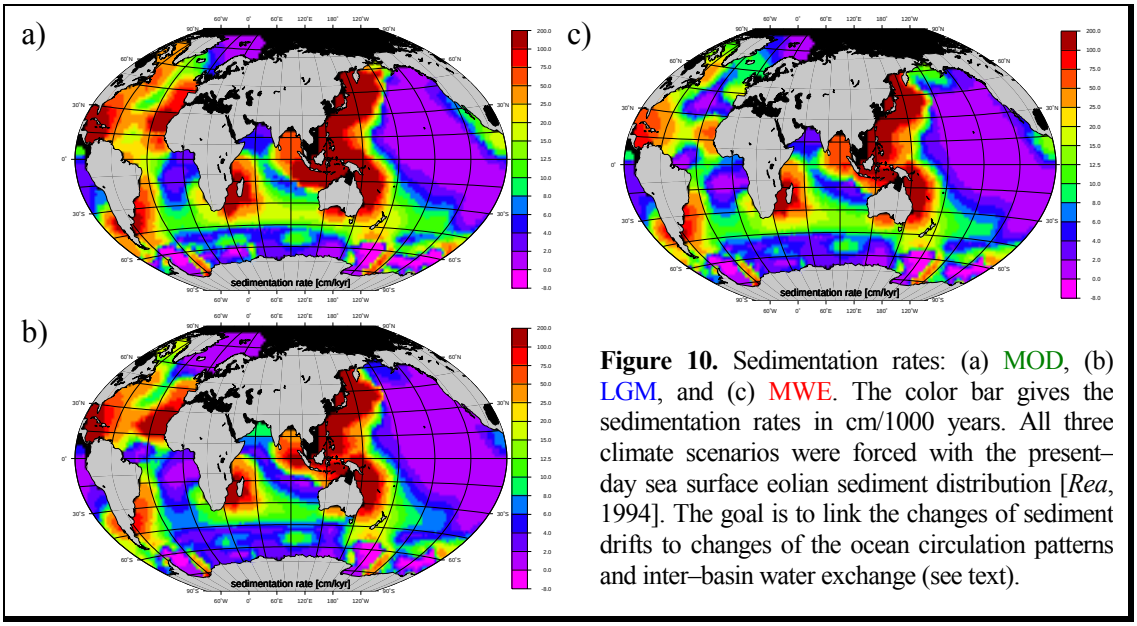

Figure 10. Sedimentation rates: (a) MOD, (b) LGM, and (c) MWE. The color bar gives the sedimentation rates in cm/1000 years. All three climate scenarios were forced with the present–day sea surface eolian sediment distribution [*Rea*, 1994]. The goal is to link the changes of sediment drifts to changes of the ocean circulation patterns and inter–basin water exchange (see text).

Sea are too low although the atmospheric dust concentration is high and the modeled circulation fits observations. A lack of correlation between the surface supply and bottom accumulation is also found in the Bay of Bengal and several other regions. In the Arabian Sea, for example, simulated sedimentation rates are, by an order of magnitude higher due to a higher eolian dust supply. However, the model sedimentation rates in the northern part of the Indian Ocean are much lower than observed. The reason for this discrepancy is the lack of strong riverine sediment input in our simulations (riverine sediment discharge is responsible at least for approximately 90% of sediment deposition [*Lisitzin*, 1996]).

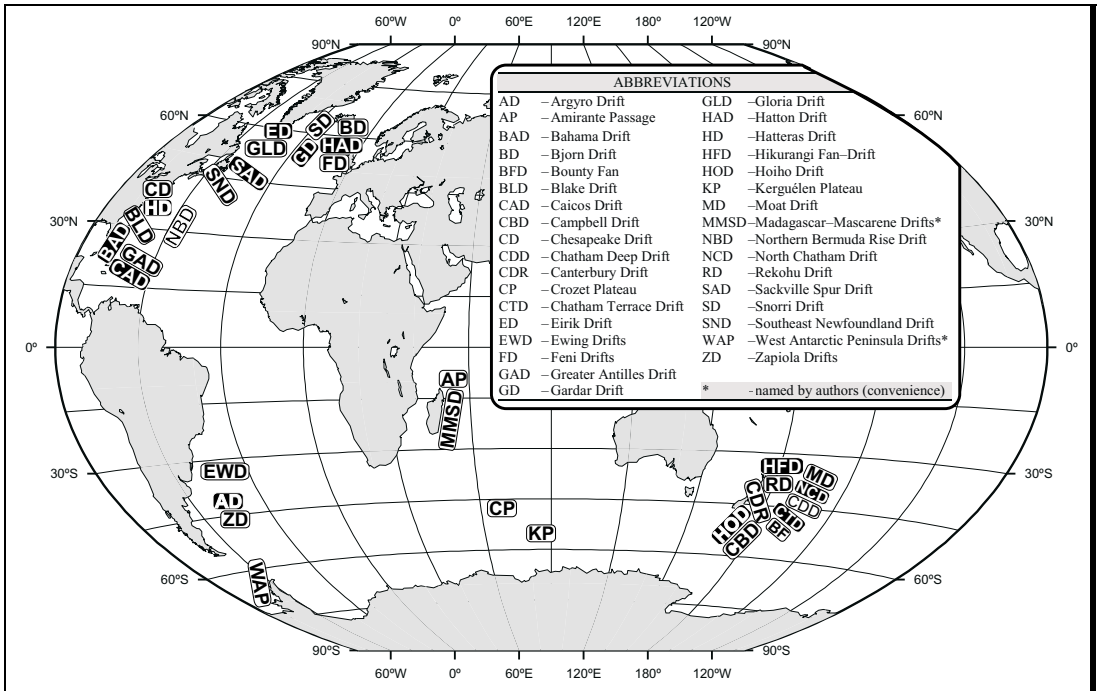

Figure 11. Locations of sediment drifts.

For the Yellow Sea and East China Sea simulated sediment distribution matches the geologic record [*Nittrouer and Wright*, 1994] qualitatively. However, the model underestimates the sediment accumulation compared to observed sedimentation rates. This discrepancy is due to the riverine inputs absent from the model. For example, there is a large supply of inorganic sediment from the Huanghe (Yellow River), which is a substantial regional source, running into the Gulf of Bohai [*Nittrouer and Wright*, 1994]. However, for modeling the large–scale open–ocean patterns this source is not essential, and the impact of deep–ocean currents can be traced more accurately. For the central North Pacific SEDLOB's predicted low sedimentation rates are consistent with measurements [*Rea et al.*, 1985] (see also e.g., *Lisitzin* [1996]). Sedimentation rates derived from their data range from a minimum of 0.02 cm/ka (30ºN) to a maximum of about 1.4 cm/ka (40ºN).

Since ice–capped Antarctica does not provide much eolian dust to the world ocean (see Figure 3), sediment deposition rates around Antarctica are relatively low [*Rea*, 1994]

(see also e.g., *Lisitzin* [1996]. Also, a part of the Southern Ocean is covered by sea ice screening the ocean from atmospheric dust. Our present–day simulations are in good agreement with these observations. Although the sediment supply around the Antarctica is low, SEDLOB predicts sediment accumulations along the continental rise west of the Antarctic Peninsula between 63 and 69ºS where *Rebesco et al.* [1994] identified several sediment mounds as drifts in the area where the currents weaken and turn northeastward. Another area with an increased sedimentation rate over a large area is beneath the Antarctic Circumpolar Current – southeast of the Crozet Plateau near the Kerguelen Plateau [*Hollister and McCave*, 1984]. These features of simulated patterns that agree well with observations can only result from deep–ocean transport. Thus, these results indicate that the deep–ocean current system is adequately modeled.

Importantly, the modeled circulation patterns reflect major glacial–interglacial climate variability introduced in the surface boundary conditions. They are substantially different in the three OGCM experiments. Since all experiments were run with the same present–day eolian surface dust distribution from *Rea* [1994], we can focus on changes in deep–sea sediment depositions caused exclusively by changes in the ocean circulation and inter–basin water exchange, rather than possible change in eolian sediment supply.

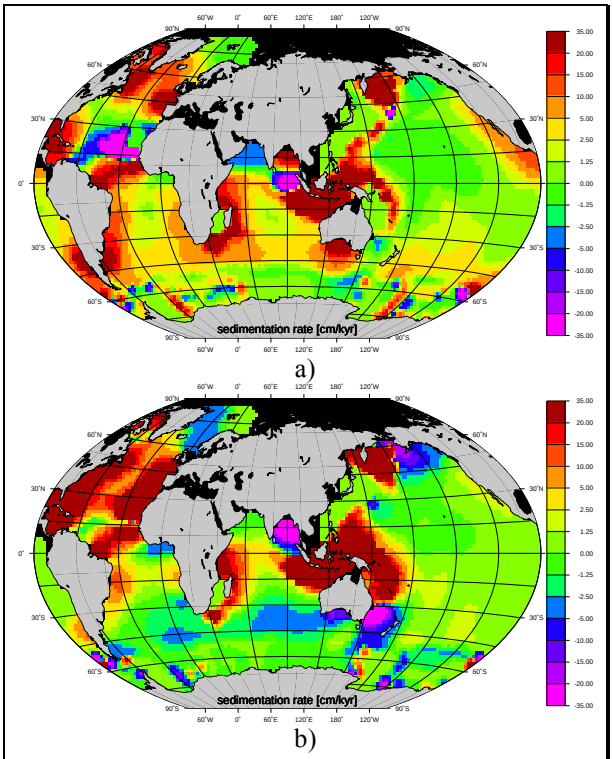

Figure 12. Differences of sedimentation rates between (a) MOD and LGM and (b) between MOD and MWE experiments. The color bar gives the scale of the thickness (in centimeters) of sediment accumulated during 1000 years, or sedimentation rates in cm kyr^{-1}.

The maps of absolute deposition rates in Figure 10 look very similar in all three sets of experiments. However, the maps of the differences between the sediment deposition rates in the LGM and MOD (Figure 12a) and MWE and MOD (Figure 12b) clearly reveal the presence of the ocean circulation impact. The strongest changes in sedimentation rates correlate well with the changes of the strongest deep–ocean currents, especially the western boundary currents (a more detailed discussion can be found in *Haupt et al.* [2001] and *Seidov et al.* [2001]). This result agrees well with deep–sea measurements (see for example *Hollister and McCave* [1984]).

Conclusions

In a set of numerical experiments, we have presented the change of the THC for three different climates, the present–day, the last glacial maximum, and the meltwater event. As ocean currents at least partially control the dynamics of sediment drifts, these drifts may be indicative of major changes in circulation patterns. Our numerical simulations allow assessment of the quality of circulation reconstructions based on their ability to produce sedimentation patterns that are comparable with the geologic record. Yet our relatively coarse–resolution experiments are rather limited in this capacity. For instance, an eddy–resolving model would yield far stronger western boundary currents – one of the key elements in circulation–sediment transport coupling. There are many other weaknesses of this study. Most obvious is the exclusion of riverine sediment discharge. Moreover, the same present–day pattern of the surface sediment source was used for all three time slices. However, despite of all these shortcomings, the link between millennial–scale changes in ocean currents and sedimentation is clearly seen and is in a reasonable agreement with the changes of sediment drift patterns. Thus, the geologic record of eolian dust accumulation can be used to verify modeled circulation patterns in scenario–type numerical simulation studies of millennial–scale and longer ocean variability. Validating the deep–ocean circulation schemes using sedimentary data can dramatically increase our confidence in modeling past climates.

Acknowledgments

We appreciate the comments by Catherine E. Stickley that helped to improve the manuscript and thank Eric J. Barron for his support. This study is partly supported by National Science Foundation (grant #9975107 and ATM 00–00545).

References

Bitzer, K. and R. Pflug, 1990: DEPOD: A three-dimensional model for simulating clastic sedimentation and isostatic compensation in sedimentary basin, In: T.A. Cross (Editor), Quantitative Dynamics Stratigraphy. Prentice Hall, N.Y., pp. 335-348.

Bohrmann, G., R. Henrich and J. Thiede, 1990: Miocene to Quaternary paleoceanography in the northern North Atlantic: Variability in carbonate and biogenic opal accumulation, In: U. Bleil and J. Thiede (Editors), Geological History of the Polar Oceans: Arctic versus Antarctic. Kluwer Academic Publications, Norwell, Massachusetts, pp. 647-675.

Broecker, W., 1991: The great ocean conveyor, Oceanography, 1: 79-89.

Broecker, W.S., 2000: Was a change in thermohaline circulation responsible for the Little Ice Age?, Proc. Nat. Acad. Sci., 97(4): 1339-1342.

Broecker, W.S. and G.H. Denton, 1989: The role of ocean atmosphere reorganizations in glacial cycles, Geochimica Cosmochimica Acta, 53: 2465-2501.

Bryan, F., 1987: Parameter sensitivity of primitive equation ocean general circulation models, Journal of Physical Oceanography, 17: 970-985.

Bryan, K., 1969: A numerical method for the study of the circulation of the world ocean, Journal of Computational Physics, 4: 347-376.

Cao, S. and I. Lerche, 1994: A quantitative model of dynamical sediment deposition and erosion in three dimensions, Computers & Geosciences, 20: 635-663.

Carter, R.M., L. Carter and I.N. McCave, 1996: Current controlled sediment deposition from the shelf to the deep ocean: The Cenozoic evolution of circulation through the SW Pacific gateway, Geologische Rundschau, 85: 438-451.

CLIMAP, 1981: Climate: Long-Range Investigation, Mapping, and Prediction (CLIMAP) Project Members, Seasonal reconstructions of the Earth's surface at the Last Glacial Maximum. Map and Chart Ser. MC-36. Geological Society of America, Boulder, Colorado, pp. 1-18.

Cox, M., 1984: A primitive equation, 3-dimensional model of the ocean, 1, Technical Report No. 1, 250 pp. Ocean Group, Geophys. Fluid Dyn. Lab., Princeton Univ., Princeton University, New Jersey.

Cox, M., 1989: An idealized model of the world ocean, Part I: The global-scale water masses, Journal of Physical Oceanography, 19: 1730-1752.

Cummins, P.F., G. Holloway and A.E. Gargett, 1990: Sensitivity of the GFDL ocean circulation model to a parameterization of vertical diffusion, Journal of Physical Oceanography, 20: 817-830.

Duplessy, J.-C., L. Labeyrie, A. Julliet-Lerclerc, J. Duprat and M. Sarnthein, 1991: Surface salinity reconstruction of the North Atlantic Ocean during the Last Glacial Maximum, Oceanologica Acta, 14: 311-324.

Ericksen, M.C., D.S. Masson, R. Slingerland and D. Swetland, 1989: Numerical simulation of circulation and sediment transport in the late Devonian Catskill Sea, In: T.A. Cross (Editor), Quantitative Dynamic Stratigraphy. Prentice Hall, Englewood Cliffs, pp. 295-305.

ETOPO5, 1986: Digital Relief of the Surface of the Earth,, National Geophysical Data Center, Boulder, Colorado.

Fairbanks, R.G., 1989: A 17,000-year glacio-eustatic sea level record: Influence of glacial melting rates on the Younger Dryas event and deep-ocean circulation, Nature, 342: 637-642.

Faugeres, J.C., M.L. Mezerais and D.A.V. Stow, 1993: Contourite drift types and their distribution in the North and South Atlantic Ocean basins, Sedimentary Geology, 82: 189-203.

Flood, R.D. and A.H. Shor, 1988: Mud waves in the Argentine Basin and their relationship to bottom circulation pattern, Part A, Deep Sea Research, 35: 943-971.

Gordon, A., 1986: Interocean exchange of thermocline water, Journal of Geophysical Research, 91: 5037-5046.

Granjeon, D. and P. Joseph, 1999: Concepts and applications of a 3D multiple lithology, diffusive model in stratigraphic modeling, In: J. Harbaugh, W.L. Watney, E.C. Rankey, R. Slingerland, R.H. Goldstein and E.K. Franseen (Editors), Numerical Experiments in Stratigraphy: Recent Advances in Stratigraphy/Sedimentologic Computer Simulations. Special publication Series #62. SEPM (Society for Sedimentary Geology)/Special Publication Series #62, Kansas, pp. 197-210.

Haupt, B.J., 1995: Numerische Modellierung der Sedimentation im nördlichen Nordatlantik, 54, Sonderforschungsbereich 313, Universität Kiel, Kiel.

Haupt, B.J., C. Schäfer-Neth and K. Stattegger, 1994: Modeling sediment drifts: A coupled oceanic circulation-sedimentation model of the northern North Atlantic, Paleoceanography, 9(6): 897-916.

Haupt, B.J., C. Schäfer-Neth and K. Stattegger, 1995: Three-dimensional numerical modeling of late Quaternary paleoceanography and sedimentation in the northern North Atlantic, Geologische Rundschau, 84: 137-150.

Haupt, B.J., D. Seidov and E.J. Barron, 2001: Glacial-to-interglacial changes of the ocean circulation and eolian sediment transport, In: D. Seidov, B.J. Haupt and M. Maslin (Editors), Oceans and rapid past and future climate changes: North-south connections. AGU, Washington, D.C., in press.

Haupt, B.J. and K. Stattegger, 1999: The ocean-sediment system and stratigraphic modeling in large basins, In: J. Harbaugh, W.L. Watney, E.C. Rankey, R. Slingerland, R.H. Goldstein and E.K. Franseen (Editors), Numerical Experiments in Stratigraphy: Recent Advances in Stratigraphy/Sedimentologic Computer Simulations. Special publication Series #62. SEPM (Society for Sedimentary Geology)/Special publication Series #62, Kansas, pp. 313-321.

Haupt, B.J., K. Stattegger and D. Seidov, 1999: SEDLOB and PATLOB: Two numerical tools for modeling climatically-forced sediment and water volume transport in large ocean basins, In: J. Harff, J. Lemke and K. Stattegger (Editors), Computerized Modeling of Sedimentary Systems. Springer, New York, pp. 115-147.

Hellerman, S. and M. Rosenstein, 1983: Normal monthly wind stress over the world ocean with error estimates, Journal of Physical Oceanography, 13: 1093-1104.

Hollister, C.D. and I.N. McCave, 1984: Sedimentation under deep-sea storms, Nature, 309: 220-225.

Honjo, S., 1996: Fluxes of particles to the interior of the open oceans, In: V. Ittekkot, P. Schäfer, S. Honjo and P.J. Depetris (Editors), Particle Flux in the Ocean. SCOPE Report 57. Chichester, Chichester, pp. 91-154.

Lehman, S.J.e.a., 1991: Initiation of Fennoscandina ice-sheet retreat during the last glaciation, Nature, 349: 513-516.

Levitus, S. and T.P. Boyer, 1994: World Ocean Atlas, vol. 3, Salinity, 99 pp., Natl. Ocean and Atmos. Admin., Washington, D. C.

Levitus, S., R. Burgett and T.P. Boyer, 1994: World Ocean Atlas, vol. 4, Temperature, 117 pp., Natl. Ocean and Atmos. Admin., Washington, D. C.

Lisitzin, A.P., 1996, Oceanic sedimentation: lithology and geochemistry. American Geophysical Union, Washington, D.C., 400 pp.

Lorenz, S., B. Grieger, H. P. and K. Herterich, 1996: Investigating the sensivity of the atmospheric general circulation Model ECHAM 3 to paleoclimate boundary conditions., Geol. Rundsch., 85: 513-524.

Maier-Reimer, E., U. Mikolajewicz and K. Hasselmann, 1991: On the sensitivity of the global ocean circulation to changes in the surface heat flux forcing, Max-Plank-Institut für Meteorologie, Hamburg, Report No. 68: 67.

Manabe, S. and R. Stouffer, 1997: Coupled ocean-atmosphere model response to freshwater input: Comparison to Younger Dryas event, Paleoceanography, 12: 321-336.

Manabe, S. and R.J. Stouffer, 1988: Two stable equilibria of a coupled ocean-atmosphere model, Journal of Climate, 1: 841-866.

Manabe, S. and R.J. Stouffer, 1995: Simulation of abrupt change induced by freshwater input to the North Atlantic Ocean, Nature, 378: 165-167.

McCave, I.N. and B.E. Tucholke, 1986: Deep current controlled sedimentation in the western North Atlantic, In: P.R. Vogt and B.E. Tucholke (Editors), The Geology of North America. The Geological Society of America, Boulder, Colorado, pp. 451-468.

Mienert, J., J.T. Andrews and J.D. Milliman, 1992: The East Greenland continental margin (65°N) since the last deglaciation: Changes in seafloor properties and ocean circulation, Marine Geology, 106: 217-238.

MOM-2, 1996: Documentation, User's Guide and Reference Manual (edited by R. C. Pacanowski), GFDL Ocean Technical Report No. 3.2, Geophysical Fluid Dynamics Laboratory/NOAA, Princeton, N.J.

Nittrouer, C.A. and L.D. Wright, 1994: Transport of particles across continental shelves, Review of Geophysics, 32(1): 85-113.

Pacanowski, R., K. Dixon and A. Rosati, 1993: The GFDL Modular Ocean Users Guide, Geophys. Fluid Dyn. Lab., Princeton Univ., Princeton, N. J.

Paola, C., P.L. Heller and C.L. Angevine, 1992: The large scale dynamics of grain–size variation in alluvial basins, 1: Theory, Basin Research, 4: 73–90.

Rahmstorf, S., 1995: Climate drift in an ocean model coupled to a simple, perfectly matched atmosphere, Climate Dynamics, 11: 447-458.

Rahmstorf, S. and M.H. England, 1997: Influence of Southern Hemisphere winds on North Atlantic Deep Water flow, Journal of Physical Oceanography, 27: 2040-2054.

Rea, D.K., 1994: The paloclimatic record provided by eolian deposition in the deep sea: The geologic history of wind, Review of Geophysics, 32(1): 159-195.

Rea, D.K., M. Leinen and T.R. Janecek, 1985: Geologic approach to the long-term history of atmospheric circulation, Science, 227: 721-725.

Rebesco, M., R.D. Larter, P.F. Barker, A. Camerlenghi and L.E. Vanneste, 1994: The history of sedimentation on the continental rise west of the Antarctic Peninsula, Terra Antarctica, 1(2): 277-279.

Ruddiman, W.F. and A. McIntyre, 1981: The mode and mechanism of the last deglaciation: Oceanic evidence., Quaternary Research, 16: 125-134.

Sarnthein, M., E. Jansen, M. Weinelt, M. Arnold, J.-C. Duplessy, H. Erlenkeuser, A. Flatoy, G. Johannessen, T. Johannessen, S. Jung, N. Koc, L. Labeyrie, M. Maslin, U. Pflaumann and H. Schulz, 1995: Variations in Atlantic Ocean paleoceanography, 50°-85°N: A time-slice record of the last 30,000 years, Paleoceanography, 10: 1063-1094.

Sarnthein, M., K. Winn, S.J.A. Jung, J.C. Duplessy, L. Labeyrie, H. Erlenkeuser and G. Ganssen, 1994: Changes in east Atlantic deepwater circulation over the last 30,000 years: Eight Time Slice Reconstructions, Paleoceanography, 9: 209-267.

Schmitz, W.J., Jr., 1995: On the interbasin-scale thermohaline circulation, Reviews of Geophysics, 33: 151-173.

Schulz, H., 1994: Meeresoberflächentemperaturen im frühen Holozän 10,000 Jahre vor heute, Dissertation Thesis, Universität Kiel, Kiel, Germany, 156 pp.

Seidov, D. and B.J. Haupt, 1997: Simulated ocean circulation and sediment transport in the North Atlantic during the Last Glacial Maximum and today, Paleoceanography, 12: 281-306.

Seidov, D. and B.J. Haupt, 1999: Last glacial and meltwater interbasin water exchanges and sedimentation in the world ocean, Paleoceanography, 14: 760-769.

Seidov, D., B.J. Haupt, E.J. Barron and M. Maslin, 2001: Ocean bi-polar seesaw and climate: Southern versus northern meltwater impacts, In: D. Seidov, B.J. Haupt and M. Maslin (Editors),

Oceans and rapid past and future climate changes: North-south connections. AGU, Washington, D.C., in press.

Seidov, D. and M. Maslin, 1999: North Atlantic Deep Water circulation collapse during the Heinrich events, Geology, 27: 23-26.

Seidov, D. and M. Maslin, 2001: Atlantic Ocean heat piracy and the bi-polar climate sea-saw during Heinrich and Dansgaard-Oeschger events, Journal of Quaternary Science, 16(4): 321-328.

Seidov, D., M. Sarnthein, K. Stattegger, R. Prien and M. Weinelt, 1996: North Atlantic ocean circulation during the Last Glacial Maximum and subsequent meltwater event: A numerical model, Journal of Geophysical Research, 101: 16305-16332.

Shanks, A.L. and J.D. Trent, 1980: Marine snow: Sinking rates and potential role in vertical flux, Deep Sea Research, 27, Part A: 137-143.

Slingerland, R., J.W. Harbaugh and K.P. Furlong, 1994, Simulating Clastic Sedimentary Basins. PTR Prentice Hall, Englewood Cliffs, 220 pp.

Stattegger, K., B.J. Haupt, C. Schäfer-Neth and D. Seidov, 1997: Numerische Modellierung des Ozean–Sediment-Systems in großen Meeresbecken: Das Spätquartär im nördlichen Nordatlantik, Geowissenschaften, 15(1): 10-15.

Stommel, H., 1958: The abyssal circulation, Deep-Sea Research, 5: 80-82.

Syvitski, J.P.M. and S. Daughney, 1992: Delta2: Delta progradation and basin filling, Computer and Geosciences, 18(7): 839-897.

Tetzlaff, D.N. and J.W. Harbaugh, 1989, Simulating Clastic Sedimentation. Van Nostrand Reinhold, New York, 202 pp.

Toggweiler, J.R., K. Dixon and K. Bryan, 1989: Simulations of radiocarbon in a coarse-resolution world ocean circulation model, 1, Steady state prebomb distribution, Journal of Geophysical Research, 94: 8217-8242.

Toggweiler, J.R. and B. Samuels, 1995: Effect of Drake Passage on the global thermohaline circulation, Deep Sea Research, 42: 477-500.

Weinelt, M., 1993: Veränderungen der Oberflächenzirkulation im Europäischen Nordmeer während der letzten 60.000 Jahre - Hinweise aus stabilen Isotopen, 41, Sonderforschungsbereich 313, Universität Kiel, Kiel.

Winguth, A., D. Archer, J.-C. Duplessy, E. Maier-Reimer and U. Mikolajewicz, 1999: Sensitivity of paleonutrient tracer distribution and deep-sea circulation to glacial boundary conditions, Paleoceanography, 14(3): 304-323.

Zanke, U., 1982, Grundlagen der Sedimentbewegung. Springer–Verlag, Berlin, Heidelberg, New York, 402 pp.